http://dx.doi.org/10.5012/bkcs.2014.35.12.3475

Systematic Analysis for the Effects of Atmospheric Pollutants in Cathode Feed on the Performance of Proton Exchange Membrane Fuel Cells

Young-Gon Yoon,[†,‡,a] Insoo Choi,[†,a] Chang-Ha Lee,[‡] Jonghee Han,[†,§] Hyoung-Juhn Kim,[†] EunAe Cho,[†] Sung Jong Yoo,[†] Suk Woo Nam,[†,§] Tae-Hoon Lim,[†] Jong Jin Yoon,[#] Sehkyu Park,[¶,*] and Jong Hyun Jang[†,§,*]

[†]*Fuel Cell Research Center, Korea Institute of Science and Technology (KIST), Seoul 136-791, Korea. [*]E-mail: jhjang@kist.re.kr*
[‡]*Department of Chemical and Biomolecular Engineering, Yonsei University, Seoul 120-749, Korea*
[§]*Green School, Korea University, Seoul 136-713, Korea*
[#]*Research & Development Division, Hyundai Motor Company, Gyeonggi-do 446-912, Korea*
[¶]*Department of Chemical Engineering, Kwangwoon University, Seoul 139-701, Korea. [*]E-mail: vitalspark@kw.ac.kr*
Received June 11, 2014, Accepted August 8, 2014

This paper describes how primary contaminants in ambient air affect the performance of the cathode in fuel cell electric vehicle applications. The effect of four atmospheric pollutants (SO_2, NH_3, NO_2, and CO) on cathode performance was investigated by air impurity injection and recovery test under load. Electrochemical analysis *via* polarization and electrochemical impedance spectroscopy was performed for various concentrations of contaminants during the impurity test in order to determine the origins of performance decay. The variation in cell voltage derived empirically in this study and data reported in the literature were normalized and juxtaposed to elucidate the relationship between impurity concentration and performance. Mechanisms of cathode degradation by air impurities were discussed in light of the findings.

Key Words : Air impurity, Performance loss, Voltage recovery, Cathode, Proton exchange membrane fuel cell

Introduction

Proton exchange membrane fuel cells (PEMFCs) are considered a promising technology to address the depletion of fossil fuels and global problems associated with the emission of greenhouse gases. Compared with conventional power sources, PEMFCs have several advantages such as rapid start-up, high power-density, long-term durability, zero emission of pollutants, high fuel-to-energy efficiency, and flexibility of reactant fuel.[1-4] For these reasons, PEMFCs have been extensively developed for fuel cell electric vehicles (FCEVs) to replace conventional internal-combustion-engine (ICE) vehicles, as well as for portable and residential applications.[4,5]

As already pointed out by many fuel cell scientists and engineers, there remain two main barriers to commercially viable FCEVs: cost-effectiveness and durability.[4-6] Recently, many studies of PEMFCs have focused on the development of inexpensive and durable materials/components in PEMFCs.[7-12] In addition, the effect of impurities in hydrogen feed has been researched mainly for the utilization of reformate gases.[13] However, the effect of atmospheric pollutants in cathode feeds, such as sulfur dioxide (SO_2), ammonia (NH_3), nitrogen dioxide (NO_2), and carbon monoxide (CO), has received less attention, even though it is considered a practical issue for the performance and durability of FCEVs. Cathode degradation/failure due to air impurities shorten the lifetime of the PEMFC stack, resulting in additional expenses for its maintenance and recovery.

[a]These authors contributed equally to this work.

The cathode degradation by air impurity is studied for automotive and stationary applications.[13,14] For stationary application, the impurity effect was investigated by measuring a decay rate upon natural exposure, for more than thousands hours, to the atmospheric contaminant of which concentration was sub ppb.[14] For automotive application, however, the impurity level is subject to be hundreds ppm.[13] Moreover, the operation time for fuel cell vehicle is within few hours, and the duration of exposure is limited. Therefore, the impurity effects seen from both cases should be distinguished and analyzed by entirely different perspectives. This study is solely focused on the automotive application.

According to national ambient air quality standards (NAAQS), the concentration of atmospheric pollutants, with 1 h-averaging time, should be less than 0.075 ppm for SO_2, 0.1 ppm for NO_2, and 0.075 ppm for CO.[15] Moreover, impurity concentrations for typical FCEV operating conditions on highways are expected to be much higher than the standard values in NAAQS, due to emissions from conventional ICEs. It has been reported that the emissions from ICEs contain 4 ppm of SO_2[16] and 6 ppm of NH_3.[17] In addition, the measured concentrations of NO_2 (28 ppm)[18] and CO (155 ppm)[19] for highway locations were much higher than NAAQS standards. Hence, it would be worthwhile to analyze the effect on fuel cell performance of various atmospheric pollutants across a wide range of concentrations. The results are expected to inform the effective design of FCEVs with an adequate air filtration system.

The influence of individual impurities on cathode performance has been investigated using various oxidants containing impurities such as SO_2,[20-24] NH_3,[23,25] NO_2,[20-23,26] and

CO.[20] For example, Moore *et al.*[20] analyzed the impurity effect of SO_2, NO_2, and CO at fixed concentrations of 500 ppb, 400 ppb, and 20 ppm, respectively. Van Zee's group[21] reported more severe degradation with higher concentration of SO_2 (5 ppm) and NO_2 (5 ppm) in air. However, most previous studies only tested selected impurities at fixed concentrations, and so their conclusions stopped short of generalizing the effects of impurities on FC performance. In addition, as the test procedures and conditions differed, it is very difficult to develop a general discussion *via* analysis of the experimental results from the various reports. Therefore, comprehensive performance measurement for major contaminants under standardized conditions is imperative for the development of practical FCEVs.

In this study, durability tests of four different impurities (SO_2, NH_3, NO_2, and CO) were conducted at concentrations from 1–100 ppm (10–1000 ppm for CO) to offer more practical data for FCEV applications in a typical road condition, through a comprehensive and comparative study. An analysis protocol was developed to evaluate the effect of contaminants on constant-current operation at 1 A/cm^2, rezpresented by polarization curves and electrochemical impedance spectroscopy (EIS). This facilitates effective analysis of apparent performance variation and polarization sources, caused by the individual contaminants at various concentrations. This systematic analysis of the effect of atmospheric pollutants is expected to provide fuel cell researchers and manufacturers with practical information on the control of on-site air feed to the cathode compartments in PEMFC stacks (*e.g.*, selective air filtering), and to further develop impurity-tolerant catalysts at the cathode.

Experimental

For single cell tests, a commercially available membrane electrode assembly (MEA) (Series 5710, Gore^{TM}, carbon-supported Pt catalyst, 0.4 mg$_{Pt}$/cm^2 at cathode and anode, 25 cm^2) was inserted into a single-cell fixture with serpentine flow channels. After its installation at a fuel cell test station, a single cell was activated under constant voltage (0.45 V) for 20 h at 65 °C. Humidified hydrogen and air were fed to the anode and cathode at a flow rate of 417 cm^3/min and 1300 cm^3/min, corresponding to stoichiometric ratios at 1.6 A/cm^2 of 1.5 and 2.0 respectively.

Electrochemical characterization of the effect of air impurities comprised three steps: reference step, poisoning step, and recovery step. To the cathode, uncontaminated air was supplied during reference and recovery steps, and air/impurity mixture gas in the poisoning step, whereas humidified hydrogen was supplied to the anode during all three steps. The flow rates for the anode (hydrogen) and cathode (air or air/impurity mixture) were controlled at 261 cm^3/min and 813 cm^3/min, corresponding to stoichiometric ratios at 1.0 A/cm^2 of 1.5 and 2.0 respectively. This study examined the effects of four air impurities: sulfur dioxide (SO_2), ammonia (NH_3), nitrogen dioxide (NO_2), and carbon monoxide (CO). Air/impurity gas mixture with a fixed air-to-impurity ratio of 9:1 was diluted by humidified air stream to give impurity concentrations of 1 ppm, 10 ppm, 100 ppm, and 1000 ppm (Figure 1). The air/impurity mixture was injected after the cathode humidifier to avoid the dissolution of impurity in the water of the humidifier, because impurity has certain degree of solubility in water: 90 g/L for SO_2, 480 g/L for NH_3 at 25 °C. The flow rate of air/impurity gas and humidified air was controlled to maintain constant total flow rate with pre-determined impurity level.

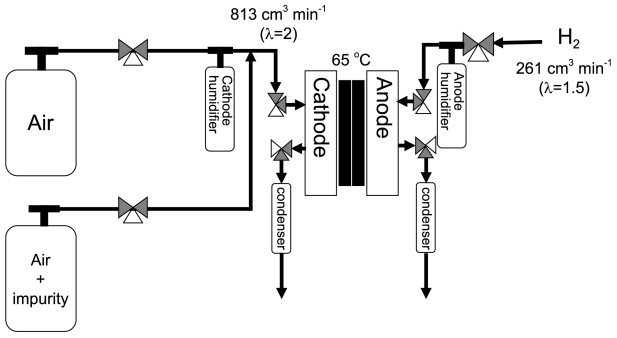

Figure 1. Schematic diagram for air impurity injection and recovery test.

The air impurity injection and recovery test comprising three steps is depicted in Figure 2. The cell was operated at 65 °C under atmospheric conditions, because the operating temperature of fuel cell for automotive application resides between 60 and 80 °C.[13,27] First, during the reference step, the cell was operated at constant current of 1 A/cm^2 for 2 h with uncontaminated air in the cathode. Then, after the contaminated cathode feed was introduced (poisoning step), an open-circuit voltage (OCV) operation (1 h) and constant-current operation (2 h) were carried out to monitor performance decay. In the recovery step, the cathode feed reverted to clean air and voltage variation was measured at 1 A/cm^2 (2 h). For each step, 15 min-polarizations were conducted before and after constant current operation (2 h). On that note, the duration of reference, poisoning, and recovery step was 2.5 h, 3.5 h, and 2.5 h, respectively, where the poisoning

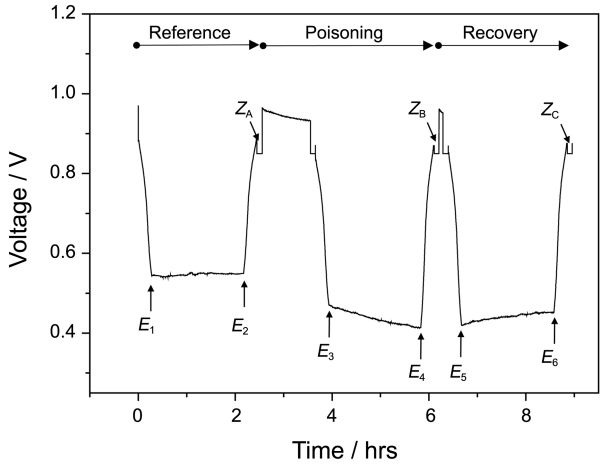

Figure 2. The sequence for measuring voltage and impedance during air impurity injection and recovery test.

step contains additional OCV operation (1 h). Therefore, the total time to evaluate the effect of specific air impurity was 8.5 h, as seen in Figure 2. The voltage decay during constant current operations was evaluated by measuring the initial and final voltages in reference (E_1 and E_2), impurity (E_3 and E_4), and recovery (E_5 and E_6) steps. In addition, EIS analysis was carried out at the end of reference step (Z_A), impurity step (Z_B), and recovery step (Z_C), where the electrode potential was 0.85 V. Electrochemical measurements were performed with a potentiostat (Bio-Logic SAS) that was automatically controlled by EC-Lab software.

Results and Discussion

Effect of SO_2 Impurity in Air. Figure 3(a) presents the initial and final cell voltages of constant current operations in reference (E_1 and E_2), impurity (E_3 and E_4), and recovery (E_5 and E_6) steps. The SO_2 concentrations were 1 ppm, 10 ppm, and 100 ppm. The difference in cell voltage between E_1 and E_2 during the reference step was approximately 5.6 mV, demonstrating that the MEA performance was fairly consistent when supplied with uncontaminated air. However, when 1 ppm and 10 ppm SO_2 were injected, the initial voltage in constant current operation (E_3) significantly declined by 113 mV and 122 mV, respectively. In the case of 100 ppm SO_2, the degradation was so severe that the cell could last for only 15 min. The results indicated that the cathode showed drastic loss of active sites with increasing SO_2 concentration under load.

The voltage variation by impurity injection during OCV should be also considered for automotive application, because the fuel cell-powered vehicles experience dynamic load during the real-life operation. Please be noted that the E_3, the initial voltage of constant current operation, represents the accumulated performance decay during OCV and polarization (current increase) operations. In addition, some may argue that the voltage decay could be partially responsible for carbon corrosion during PEMFC operation, especially at OCV. The carbon corrosion is another factor which degrades cathode of PEMFC, however, it takes place when the voltage exceeds 1.2 V or beyond, which is out of range in this study. Therefore, the effect of the carbon corrosion on the degradation should not be considered.

Meanwhile, the cell voltages with the recovery phase (E_5 and E_6) were lower than those measured before the poisoning for 1 ppm and 10 ppm SO_2. In other words, the voltages never reached the values recorded during the reference step. From the results, it was noted that, following cathode contamination by even low concentrations of SO_2, the cell performance barely recovered despite the subsequent reintroduction of uncontaminated air to the cathode.

From the final cell voltage at each step (E_2, E_4, and E_6), the maximum performance decay (ΔE_{max}) and unrecoverable performance decay (ΔE_{unr}) were calculated *via* Eqs. (1) and (2) and plotted as a function of impurity concentration in Figure 3(b).

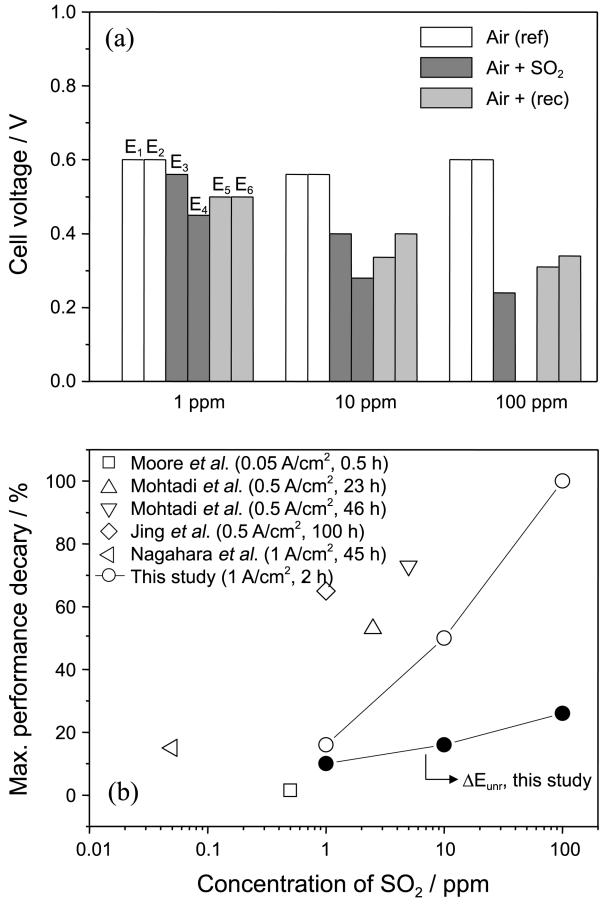

Figure 3. (a) Variation in cell voltage interrupted by SO_2; (b) Comparison of performance decay ratio.

$$\Delta E_{max} = [(E_2\text{-}E_4)/E_2] \times 100\ (\%) \quad (1)$$

$$\Delta E_{unr} = [(E_2\text{-}E_6)/E_2] \times 100\ (\%) \quad (2)$$

For comparison, Figure 3(b) shows values of ΔE_{max} from experimental data in the literature together with ΔE_{max} from the present study. For the results reported by Moore *et al.*,[20] the maximum cell performance decay with 0.5 ppm SO_2 (0.05 A/cm^2 and 0.5 h duration) was found to be on the trend line for this study (indicated by □). In contrast, the values for maximum cell performance decay ratio reported by Mohtadi *et al.*[21] (△ and ▽), Jing *et al.*[22] (◇), and Nagahara *et al.*[23] (◁) were relatively high, probably due to longer exposure time to SO_2 (> 23 h).

The voltage decay associated with SO_2 contamination can be explained by the poisoning of Pt active sites in the presence of SO_2. The adsorption of sulfur species on Pt catalysts in MEA was experimentally supported by the CV analysis with single cell in the presence of SO_2: the decreased hydrogen stripping charge[22] and oxidation peaks for adsorbed sulfur species.[21,28] In addition, the strong adsorption of SO_2 on polycrystalline Pt was confirmed by Fourier transform infrared spectroscopy (FTIR).[29] Accordingly, the voltage increase during recovery step (E_4–E_6) contributed to the partial recovery of Pt active surface with SO_2 desorption. It

was suggested that in a highly humidified atmosphere with O_2 supply, adsorbed SO_2 can be readily converted into H_2SO_4 and washed away *via* the reaction shown below:[22]

$$2Pt\text{-}SO_2 + O_2 \rightarrow 2Pt\text{-}SO_3 \quad (3)$$

$$Pt\text{-}SO_3 + H_2O \rightarrow H_2SO_4 + Pt \quad (4)$$

When the cathodic overpotential became very large, it was proposed that SO_2 can be electrochemically reduced to S on Pt surface, based on the cathodic peak at 0.21 V in linear sweep test (*vs.* RHE).[30] It was reported that the electrochemical oxidation of S_{ad} to sulfate in aqueous phase required potential cycling up to 1.5 V,[24] suggesting that the reactivation of Pt surface by electrochemical desorption of S_{ad} was very difficult in typical PEMFC operating conditions. Therefore, in this study it seemed that the Pt surface blocked by S_{ad} with significant voltage decay at high SO_2 concentration was not fully recovered, because the cell voltage was maintained below 1.0 V, which probably resulted in incomplete recovery of cell voltage as shown in Figure 3(b) (indicated by ●).

Effect of NH_3 Impurity in Air. The effect of NH_3 on the PEMFC cathode was previously reported only for a fixed concentration of 5 ppm[23] and 48 ppm,[25] while the effect on the anode has been reported for wide range of concentration (13-1000 ppm) by several research groups.[31-33] In this study, three simulated air mixtures with various NH_3 contents (1 ppm, 10 ppm, and 100 ppm) were employed to examine the effect of NH_3 contamination across a wide range of concentration on the electrochemical behavior of the PEMFC cathode. Figure 4(a) depicts the variation in cell voltage during reference, poisoning, and recovery steps with NH_3 contamination. At low NH_3 concentration (1 ppm), no variation in cell voltage was observed, whereas the same amount of SO_2 induced significant performance decay. However, as NH_3 concentration increased to 10 ppm and 100 ppm, the impurity effect became very clear and the cell voltages at 1 A/cm^2 significantly decreased. In Figure 4(b), the decay in cathode performance is presented as a function of NH_3 impurity. Compared to this study, the degradation reported by Nagahara *et al*.[23] and Garzon *et al*.[25] was smaller probably due to the shorter exposure time (0.5 h and 1 h, respectively).

The effect of NH_3 impurity has been reported to be closely related to the decrease in the conductivity of proton exchange membrane (PEM)[25,31,32] and ionomers in catalyst layer.[31,32] For example, Uribe *et al*.[31] confirmed the increase in ohmic resistance by impedance technique after injecting 30 ppm of NH_3 to anode for 3 h. They proposed that NH_4^+ ions, which are produced by the protonation of NH_3, can replace protons in the membrane electrolyte and/or ionomers in catalyst layers, resulting in the increase of ohmic resistance and the decrease in cell voltage. The conductivity decrease with NH_4^+ has been experimentally reported for Nafion membranes.[34,35] When the uncontaminated air was supplied to NH_3-exposed single cells, the cell voltage was partially recovered, probably through the disproportionation

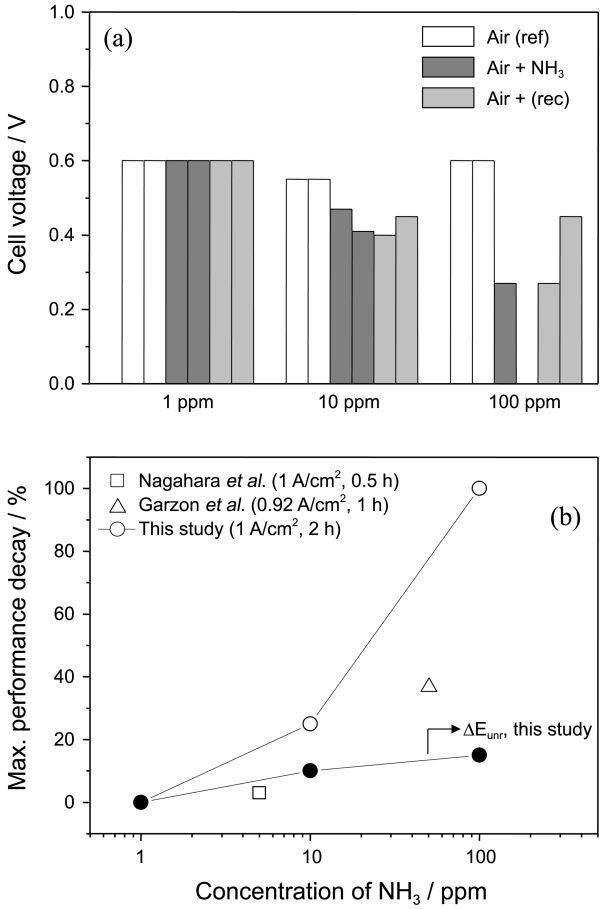

Figure 4. (a) Variation in cell voltage interrupted by NH_3; (b) Comparison of performance decay ratio.

of NH_4^+ into protons and NH_3 as reported by Nagahara *et al*.[25]

Effect of NO_2 Impurity in Air. It is well known that NO_2, a main contributor to air pollution that causes smog and acid rain, is primarily produced from ICEs where oxygen and nitrogen in the air react at high temperature. Therefore, during operation, exposure of the cathode in FCEVs to NO_2 is unavoidable in the presence of conventional ICE vehicles. Figure 5(a) presents the dependence of cell voltage on NO_2 concentration through NO_2 impurity injection and recovery test. No decay in performance is detected at low impurity level of 1 ppm, but the decay gradually increased with higher NO_2 concentration. However, unlike SO_2 and NH_3 in the air, no complete potential decay is observed at 100 ppm. Rather, the cathode showed relatively robust recovery against NO_2 poisoning.

In Figure 5(b), it appeared the maximum performance decay ratio in this study was in line with the data reported by Yang *et al*.[26] who exposed the cathode to NO_2 for a relatively short duration. Meanwhile, relatively long impurity inflow to the cathode (Mohtadi[21] and Jing[22]) resulted in a drastic decay of cathode performance. Regarding the performance decay with NO_2 impurity in cathode feeds, Mohtadi *et al*. reported that, based on the CV analysis, there was no Pt poisoning by adsorption of NO_2 species, and therefore

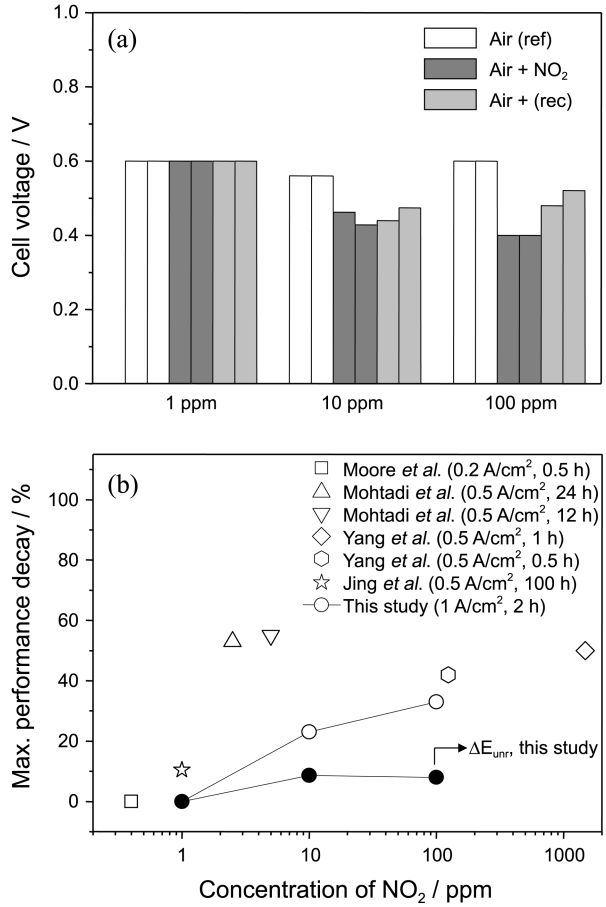

Figure 5. (a) Variation in cell voltage interrupted by NO_2; (b) Comparison of performance decay ratio.

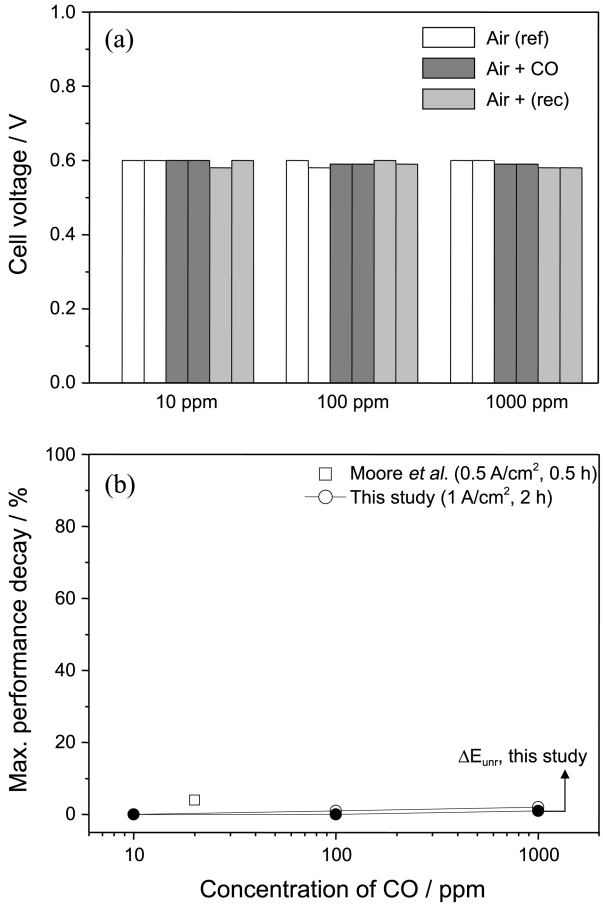

Figure 6. (a) Variation in cell voltage interrupted by CO; (b) Comparison of performance decay ratio.

supposed that the increase of ohmic resistance was the main degradation mechanism, where NO_2 was electrochemically reduced into NH_4^+.[21]

Effect of CO Impurity in Air. It is generally accepted that CO preferentially and strongly adsorbs onto Pt surface. Therefore, when CO is contained in fuel feeds to anodes, the electrochemical surface area in Pt nanoparticles drastically reduces, as demonstrated experimentally by various authors.[27,36,37] However, when CO was introduced in the air feed to cathodes, the voltage decrease by CO poisoning was found to be very small (Figure 6(a)), which is in agreement with results at 20 ppm CO reported previously.[20] Accordingly, the performance decay ratio was very low, demonstrating that the effect of CO in air feed is practically negligible (Figure 6(b)).

It is believed that CO adsorbed onto Pt catalysts in the cathode is quickly oxidized to gaseous CO_2, resulting in no significant deleterious effect on catalytic active sites even at 1000 ppm CO. As the electrode potential of the cathode is about 0.6 V, in this study at 1 A/cm^2, electrochemical oxidation of the adsorbed CO molecules is expected to be very rapid to maintain a free Pt active surface area, while the electrochemical oxidation of CO molecules is known to start at ~0.3 V *vs.* RHE in aqueous electrolyte.[38] Thus, as the operating voltage range was above 0.5 V in this study, CO in the cathode seems to have little influence on PEMFC performance.

Polarization Curves and EIS Analysis. Figure 7 shows the polarization curves during poisoning step with 10 ppm of various impurities. As seen, the characteristics of the SO_2 polarization curve differed with NH_3 and NO_2 polarization curve, which tells the origin of degradation was different. Of note, the voltages at 1.0 A/cm^2 in the polarization curves corresponded to the E_3 values in Figures 3(a), 4(a), 5(a), and 6(a). As the overpotential at low current density was greater for SO_2, it can be concluded that the Pt poisoning effect was more significant compared to that for NH_3 and NO_2, which was in agreement with the discussion in previous sections. The cell degradation by NO_2 was similar to the NH_3, and the effect of CO impurity was found to be negligible.

To confirm the major mechanism of each air impurity, EIS analysis was carried out throughout the reference, impurity, and recovery steps. Please be noted that, due to the current limitation of the used potentiostat, the EIS measurement was performed at a dc potential of 0.85 V and utilized only to evaluate the variation of ohmic resistance (R_{ohm}), whereas the cell voltages at 1 A/cm^2 was around 0.4 V. As the formation of NH_4^+ *via* protonation of NH_3 is expected to be enhanced by higher current (large amount of proton supply), the R_{ohm} variation analyzed at 0.85 V can be assumed to be

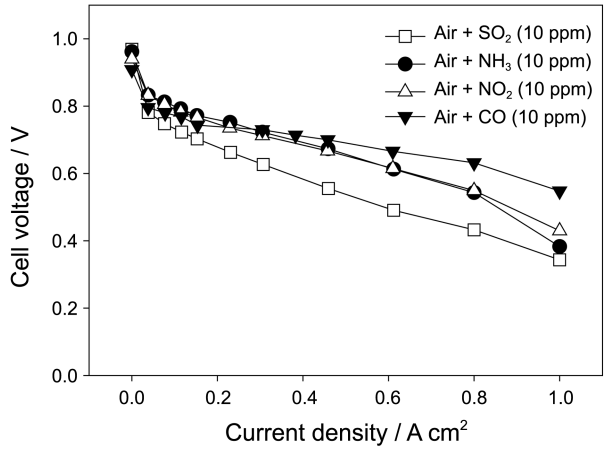

Figure 7. Polarization curves for PEMFCs with air impurities (10 ppm) of SO_2, NH_3, NO_2 and CO.

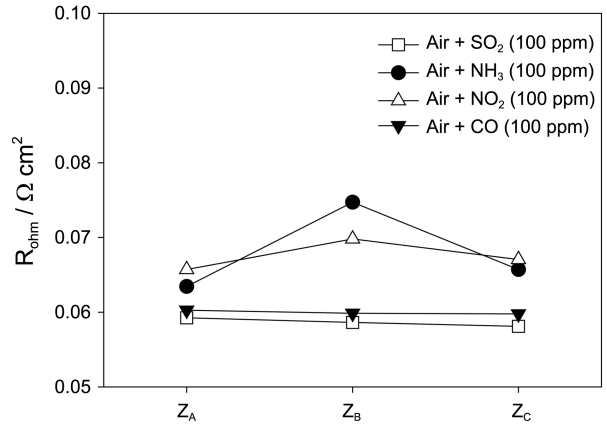

Figure 8. Ohmic resistance variations with cathode impurities (100 ppm) at a dc potential of 0.85 V.

much smaller than the actual variation during constant current operation (1 A/cm^2).

In Figure 8, the R_{ohm} values, which were determined from the high-frequency intercepts in experimental Nyquist plots, was provided for four air pollutants at a concentration of 100 ppm. It can be noticed that R_{ohm} at 0.85 V was significantly increased by NH_3 and NO_2 impurities, suggesting that the decrease in proton conductivity by NH_4^+ formation. In the case of SO_2 impurity, the change in R_{ohm} was insignificant, indicating that the performance decay was mainly due to the catalyst poisoning.

Conclusion

In this study, effect of four major pollutants in ambient air (*i.e.*, SO_2, NH_3, NO_2, and CO) on PEMFC performance was examined through air impurity injection to cathodes followed by recovery test. At higher concentration, the impurity effect on voltage degradation gradually increased for SO_2, NH_3 and NO_2, whereas CO induced practically no effect. At a concentration of 10 ppm, the degradation was most severe for SO_2 impurity (ca. 50%) compared with NH_3 and NO_2. At 100 ppm, both SO_2 and NH_3 severely degraded the PEMFC single cell, which was ascribed to Pt poisoning and PEM degradation with NH_4^+ formation, respectively, based on the literature and experimental data obtained in this study. When uncontaminated air was supplied again, the voltage recovery was found to be incomplete, due to the combined effect of irreversible degradation and insufficient recovery time. The systematic analysis in this study is expected to provide practical information for the design and control of PEMFC stacks, while further detailed investigation is also required, focusing on selected impurity condition.

Acknowledgments. This work was supported by the New & Renewable Energy Core Technology Program of the Korea Institute of Energy Technology Evaluation and Planning (KETEP) funded by the Korean Ministry of Trade, Industry & Energy (No. 20133030011320), the National Research Foundation of Korea Grant funded by the Korean Government (MSIP) (2014, University-Institute cooperation program), and the NRF grant funded by MSIP, Korea (2014R1A2A2A04003865). This work was also financially supported by KIST through Institutional Program and K-GRL program; and by the research grant of Kwangwoon University in 2014.

References

1. O'hayer, R. P.; Cha, S.-W.; Colella, W.; Prinz, F. B. *Fuel Cell Fundamentals*; John Wiley& Sons Ltd.; New York, 2006.
2. Larminie, J.; Dicks, A. *Fuel Cell System Explained*; John Wiley & Sons Ltd.; West Sussex; England, 2000.
3. Prater, K. B. *J. Power Sources* **1994**, *51*, 129.
4. Wang, Y.; Chen, K. S.; Misher, J.; Cho, S. C.; Adroher, X. C. *Appl. Energy* **2011**, *88*, 981.
5. Barbir, F. *PEM Fuel Cells: Theory and Practice*, 1st ed.; Elesevier Academic Press: New York, 2005.
6. Helmot, R.; Eberle, U. *J. Power Sources* **2007**, *165*, 833.
7. Bashyam, R.; Zelenay, P. *Nature* **2006**, *443*, 63.
8. Lefevre, M.; Proietti, E.; Jaouen, F.; Dodelet, J.-P. *Science* **2009**, *324*, 71.
9. Jaouen, F.; Proietti, E.; Lefevre, M.; Chenitz, R.; Dodelet, J.-P.; Wu, G.; Chung, H. T.; Johnston, C. M.; Zelenay, P. *Energ. & Environ. Sci.* **2011**, *4*, 114.
10. Huang, S.-Y.; Ganesan, P.; Park, S.; Popov, B. N. *J. Am. Chem. Soc.* **2009**, *131*, 13898.
11. Antolini, E. *ACS Catal.* **2014**, *4*, 1426.
12. Pascone, P.-A.; Berk, D.; Meunier, J.-L. *Catal. Today* **2013**, *211*, 162.
13. Borup, R.; Meyers, J.; Pipovar, B.; Kim, Y. S.; Mukundan, R.; Garland, N.; Myers, D.; Wilson, M.; Garzon, F.; Wood, D.; Zeleny, P.; More, K.; Stroh, K.; Zawodzinski, T.; Boncella, J.; McGrath, J. E.; Inaba, M.; Miyatake, K.; Hori, M.; Ota, K.; Ogumi, Z.; Miyata, S.; Nishikata, A.; Siroma, Z.; Uchimoto, Y.; Yasuda, K.; Kimijima, K.; Iwashita, N. *Chem. Rev.* **2007**, *107*, 3904.
14. Verhage, A. J. L.; Coolegem, J. F.; Mulder, M. J. J.; Yildirim, M. H.; De Bruijn, F. A. *Int. J. Hydrogen Energ.* **2013**, *38*, 4714.
15. National Ambient Air Quality Standards. U.S. Environmental Protection Agency. 2007, http://www.epa.gov/air/criteria.html. Accessed July 2013.
16. Lee, C.; Richer, A.; Lee, H.; Kim, Y. J.; Burrows, J. P.; Lee, Y. G.; Choi, B. C. *Atmos. Environ.* **2008**, *42*, 1461.
17. Harkins, J. H.; Nicksic, S. W. *Environ. Sci. Technol.* **1967**, *1*(9), 751.

18. Torp, C.; Larssen, S. *Sci. Total. Environ.* **1996**, *189/190*, 35.
19. Murena, F.; Garofalo, N.; Favale, G. *Atmos. Environ.* **2008**, *42*, 8204.
20. Moore, J. M.; Adcock, P. L.; Lakeman, J. B.; Mepsted, G. O. *J. Power Sources* **2000**, *85*, 254.
21. Mohtadi, R.; Lee, W.-K.; Van Zee, J. W. *J. Power Sources* **2004**, *138*, 216.
22. Jing, F.; Hou, M.; Shi, W.; Fu, J.; Yu, H.; Ming, P.; Yi, B. *J. Power Sources* **2007**, *166*, 172.
23. Nagahara, N.; Sugawara, S.; Shinohara, K. *J. Power Sources* **2008**, *182*, 422.
24. Fu, F.; Hou, M.; Du, C.; Shao, Z.; Yi, B. *J. Power Sources* **2009**, *187*, 32.
25. Garzon, F. H.; Lopes, T.; Rockward, T.; Sansinena, J.-M.; Kienitz, B.; Mukundan, R.; Springer, T. *ECS Trans.* **2009**, *25*(1), 1575.
26. Yang, D.; Ma, J.; Xu, L.; Wu, M.; Wang, H. *Electrochim. Acta* **2006**, *51*, 4039.
27. Balasubramanian, B.; Barbir, F.; Neutzler, J. 1999, http://web.anl.gov/PCS/acsfuel/preprint%20archive/Files/44_4_NEW%20ORLEANS_00-99_0977.pdf. Accessed 27 Nov 2013
28. Cheng, X.; Shi, Z.; Glass, N.; Zhang, L.; Zhang, J.; Song, D.; Liu, Z.-S.; Wang, H.; Shen, J. *J. Power Sources* **2007**, *165*, 739.
29. Quijada, C.; Rodes, A.; Vazquez, J. L.; Perez, J. M.; Aldaz, A. *J. Electroanal. Chem.* **1995**, *394*, 217.
30. Contractor, A. Q.; Lal, H. *J. Electroanal. Chem.* **1978**, *93*, 99.
31. Uribe, F. A.; Gottesfeld, S.; Zawodzinski, T. A. *J. Electrochem. Soc.* **2002**, *149*(3), A293.
32. Soto, H. J.; Lee, W.-K.; Van Zee, J. W.; Murthy, M. *Electrochem. Solid St.* **2003**, *6*(7), A133.
33. Halseid, R.; Vie, P. J. S.; Tunold, R. *J. Power Sources* **2006**, *154*, 343.
34. Halseid, R.; Vie, P. J. S.; Tunold, R. *J. Electrochem. Soc.* **2004**, *151*(3), A381.
35. Hongsirikarn, K.; Goodwin, J. G.; Greenway, S.; Creager, S. *J. Power Sources* **2010**, *195*, 30.
36. Springer, T. E.; Rockward, T.; Zawodzinski, T. A.; Gottesfeld, S. *J. Electrochem. Soc.* **2001**, *148*(1), A11.
37. Bauman, J. W.; Zawodzinski, T. A., Jr.; Gottesfeld, S. In *Proton Conducting Membrane Fuel Cells II, The Electrochemical Society Proceedings Series*; Gottesfeld, S., Fuller, T., Eds.; Pennington, NJ, 1999; 98-27, p 136.
38. Arenz, M.; Mayhofer, K. J. J.; Stamenkovic, V.; Blizanac, B. B.; Tomoyuki, T.; Ross, P. N.; Markovic, N. M. *J. Am. Chem. Soc.* **2005**, *127*, 6819.